Determining transport coefficients for a microscopic simulation of a hadron gas

Scott Pratt, Alexander Baez, and Jane Kim

Phys. Rev. C **95**, 024901 — Published 3 February 2017

DOI: 10.1103/PhysRevC.95.024901

Determining Transport Coefficients for a Microscopic Simulation of a Hadron Gas

Scott Pratt,[1] Alexander Baez,[1,2] and Jane Kim[1]

[1] *Department of Physics and Astronomy and National Superconducting Cyclotron Laboratory, Michigan State University, East Lansing, Michigan 48824, USA*

[2] *Department of Physics, University of South Florida, 4202 East Fowler Ave, Tampa, Florida 33620-7100*

(Dated: January 13, 2017)

Quark-Gluon plasmas produced in relativistic heavy-ion collisions quickly expand and cool, entering a phase consisting of multiple interacting hadronic resonances just below the QCD deconfinement temperature, $T \sim 155$ MeV. Numerical microscopic simulations have emerged as the principal method for modeling the behavior of the hadronic stage of heavy-ion collisions, but the transport properties that characterize these simulations are not well understood. Methods are presented here for extracting the shear viscosity, and two transport parameters that emerge in Israel-Stewart hydrodynamics. The analysis is based on studying how the stress-energy tensor responds to velocity gradients. Results are consistent with Kubo relations if viscous relaxation times are twice the collision time.

I. INTRODUCTION

The theory of strong interactions, QCD, predicts that at temperatures exceeding $T_c \simeq 155$ MeV, ordinary hadrons dissolve into their constituents creating a state of matter called the quark-gluon plasma (QGP). From first-principle lattice QCD studies, it is known that the transition from confined quarks and gluons (hadrons) to the deconfined quark-gluon plasma is not a true sharp phase transition but rather an analytic cross-over transition [1, 2]. Relativistic heavy-ion collisions, conducted at different collision energies at the Relativistic Heavy-Ion Collider (RHIC) and at the Large Hadron Collider (LHC) aim at understanding the properties of QCD matter by creating quark-gluon plasmas at temperatures up to ~ 450 MeV, which then expand and cool to temperatures close to T_c within a time of $\tau_0 \sim 5-10$ fm/c (10^{-22} seconds). Below T_c, quarks and gluons confine into color-neutral objects (hadrons and hadron resonances) in a process called hadronization which is still not well understood. This hadron gas then continues to expand and cool, with the different hadrons scattering, decaying and merging for $\sim 10-20$ fm/c, before the remaining particles cease to interact and are eventually recorded by the experimental detectors. With the exception of direct photons and dileptons, all experimental information on the transport properties of hot QCD matter must be extracted through detailed comparisons of models, typically centered around viscous hydrodynamics, to observations of final-state hadrons. One of the most remarkable results from analyses of RHIC data has been the inference of low shear viscosity, mainly from elliptic flow measurements [3, 4]. Recently extracted values for the shear viscosity [5–7] have ranged typically from one to four times the AdS/CFT value, where the shear viscosity to entropy ratio is $\eta/s = 1/4\pi$ [8].

From the moment the nuclei first overlap, until the last particle interaction, systems created in heavy-ion collisions spend most of their lifetime in the hadronic gas phase. As such, inferring properties of the quark-gluon plasma phase from the measured particle spectra and correlations with good precision naturally requires a solid understanding of the properties of the hadron resonance gas. Lattice gauge theory has provided estimates of the viscosity for pure gauge theory [9–12], but the uncertainty of such estimates are difficult to quantify due to the analytic continuation of correlations in imaginary time, which are readily extracted from lattice calculations, to real time, which are what is needed for the Kubo relation that gives the viscosity. Perturbative QCD also provides estimates of the viscosity [13], but such calculations can be questionable for lower temperatures near the phase transition. For the hadronic phase, calculations for a pion gas, [14–21], or for Nambu-Jona-Lasinio models [22], or for the linear sigma model [23], can provide well justified predictions for transport coefficients at lower density, where the matter is well described by pions interacting in a binary fashion, but they are not reasonable for temperatures $\gtrsim 150$ MeV. At these temperatures a plethora of excited hadronic states become significantly populated, and their interactions with one another are poorly understood.

The standard modeling procedure in heavy-ion collisions (which will also be used here) employs so-called hadron cascade codes to describe the hot hadron gas, which essentially consist of a kinetic theory simulation including all the hadronic resonance states found in the particle data book [24]. Despite residual uncertainty in this model, which arises from poorly known cross sections involving excited hadrons, this approach is considered the best current available model. In previous works attempting to extract the value of shear viscosity over entropy density η/s in a hadron gas, one study used the collision event generator URASIMA [25] and two studies used a hadron cascade code (URQMD, Ref. [26]), using different techniques [27, 28]. Of particular relevance to this study are the viscosities extracted in [27], which analyzed URQMD which is extremely similar to the hadronic cascade considered here. In that case relaxation times for the shear tensor were extracted from a static box geome-

try, which through the Kubo relation for shear viscosity provided what should be a reliable statement of the viscosity. This is the same technique that has been applied to extract the viscosity of partonic cascades for massless particles [29]. However, the results from [27] were puzzling as the extracted values of η/s did not fall with increasing temperature as one would expected given the expected fall of the collision time with increasing temperature. For massless particles with isotropic interactions there exist analytic solutions [30], but for a hadron gas some species are highly relativistic whereas others are quite non-relativistic, and the interactions often involve the creation and decay of resonances. This makes analytic approaches difficult. Due to the uncertainties in cross sections, and due to the unknown nature of multiparticle interactions, any estimate of the viscosity from these models is not to be trusted to within several tens of percent. Nonetheless, such an estimate might currently represent the field's best estimate, until a rigorous nonperturbative QCD calculation is performed. Even if the true viscosity were well known, it is also critical to understand the viscous properties of hadronic simulations so that they might be adjusted to fit desired values.

The present work is meant to improve our understanding of the hot hadron gas by providing procedures to extract transport properties from hadron cascades, and discuss findings in relation to our knowledge about transport in hot nuclear matter. One goal is to examine the stress-energy tensor to reliably extract effective viscosities and related shear transport coefficients, and to see whether the high values of the viscosity reported in [27] are reproduced. A second goal is to test whether the extracted viscosities are independent of the size of the imposed velocity gradients, which should be true for small velocity gradients, but has never been demonstrated for velocity gradients whose magnitudes are characteristic of those encountered in heavy-ion collisions. For higher velocity gradients it becomes important to consider higher-order transport coefficient such as those found in Israel-Stewart theories. The application and extension of Israel-Stewart theories in [31–34] is especially relevant to heavy-ion collisions, where super-luminar modes can emerge if the equations are parabolic. Some terms for higher-order gradient expansions can also be addressed through Kubo relations [35].

II. METHODOLOGY AND RESULTS

First, we consider the operational definition of shear viscosity from the Navier-Stokes (NS) equation,

$$T_{ij} = P\delta_{ij} - \zeta\nabla\cdot v - \eta(\partial_i v_j + \partial_j v_i - 2\nabla\cdot v/3), \quad (1)$$

where P is the equilibrated pressure for the local energy density, and η and ζ are the shear and bulk viscosities respectively. We will neglect the bulk viscosity for the moment and set $\zeta = 0$. By analyzing a hadronic simulation with a chosen velocity gradient, one can observe the behavior of the stress-energy tensor, which should be altered proportional to the shear viscosity multiplied by the velocity gradient.

On short time scales, the stress-energy tensor can be initialized to a broad range of values by adjusting the momenta of the simulated hadrons. For example, T_{zz} can be initialized to zero if the particles are set with zero longitudinal velocity in the frame moving with the average fluid velocity. In Israel-Stewart (IS) hydrodynamics, see appendix, the deviations of the stress-energy tensor, $T_{ij} - P\delta_{ij}$, are dynamical variables that relax toward their Navier-Stokes values. Defining $\pi_{zz} \equiv T_{zz} - P$, the IS equations are

$$\begin{aligned}\partial_t \pi_{ij} &= -\frac{1}{\tau_\pi}\left(\pi_{ij} - \eta\omega_{ij}\right) - \gamma_\pi \omega_{ik}\pi_{kj} - \kappa_\pi \nabla\cdot v\pi_{ij},\\ \omega_{ij} &\equiv \partial_i v_j + \partial_j v_i - (2/3)\delta_{ij}\nabla\cdot v. \end{aligned} \quad (2)$$

The dimensionless coefficients κ_π and γ_π can depend on the temperature. For a massless gas with fixed cross sections and isotropic scatterings, kinetic theory gives the coefficients as $\kappa_\pi = 4/3$ and $\gamma_\pi = 5/7$ [33, 36–39]. The coefficient κ_π can be related to fluctuations of the stress-energy tensor, F_π (see appendix).

$$\begin{aligned}\kappa_\pi &= s\frac{\partial_s \alpha}{\alpha},\\ \alpha^2 &= F_\pi s. \end{aligned} \quad (3)$$

Here, s is the entropy density and F_π is the equal-time fluctuation of the traceless elements of the stress-energy tensor and is related to the viscosity and the relaxation time τ_π through a Kubo relation,

$$\begin{aligned}\eta &= \frac{1}{2T}\int d^4 r\ \langle T_{xy}(0)T_{xy}(r)\rangle \quad (4)\\ &\approx \frac{\tau_\pi}{T}F_\pi,\\ F_\pi &= \sum_i (2S_i+1)\int \frac{d^3p}{(2\pi)^3}\frac{p_x^2 p_y^2}{E_i(\mathbf{p})^2}e^{-E_i(\mathbf{p})/T} \quad (5)\\ &= \sum_i (2S_i+1)\frac{1}{15}\int \frac{d^3p}{(2\pi)^3}\frac{p^4}{E_i(\mathbf{p})^2}e^{-E_i(\mathbf{p})/T},\\ \frac{F_\pi}{T} &= P - \frac{1}{15}\sum_i (2S_i+1)\int \frac{d^3p}{(2\pi)^3}\frac{p^4}{E_i(\mathbf{p})^3}e^{-E_i(\mathbf{p})/T}. \end{aligned}$$

Here, the expression with τ_π implies that correlations decay exponentially with time characterized by a single decay time, τ_π. This assumption is implicit in the IS approach. Other thermodynamic quantities, such as the pressure, energy density and entropy density can also be expressed as integrals over momentum,

$$\begin{aligned}P &= \sum_i (2S_i+1)\int \frac{d^3p}{(2\pi)^3}\frac{p^2}{3E_i(\mathbf{p})}e^{-E_i(\mathbf{p})/T}, \quad (6)\\ &= \frac{m^2T^2K_0(m_i/T) + 2m_iT^3K_1(m_i/T)}{2\pi^2},\\ \epsilon &= \sum_i (2S_i+1)\int \frac{d^3p}{(2\pi)^3}E_i(\mathbf{p})e^{-E_i(\mathbf{p})/T}, \end{aligned}$$

$$s = \frac{P+\epsilon}{T}.$$

The expressions for F_π, P, ϵ and s assume that hadrons behave as a gas, i.e. the only correlations at equal times are those between a particle and itself. Lacking a simple analytic formula for the integral for F_π for relativistic but massive particles, that integral was performed numerically, whereas analytic expressions were used for the other thermodynamic quantities. After performing the integrals listed above, one can then determine κ_π from Eq. (3),

$$\begin{aligned}\kappa_\pi &= s\frac{\partial_s (F_\pi s)^{1/2}}{(F_\pi s)^{1/2}} \\ &= \frac{1}{2} + \frac{1}{2}\frac{(1/F_\pi)\partial_T F_\pi}{(1/s)\partial_T s}.\end{aligned} \tag{7}$$

For massless particles $F_\pi \sim T^5$ and $s \sim T^3$, so $\kappa_\pi = 4/3$. For the case $m >> T$, $\kappa_\pi \to 1$. For the range of temperatures, $100 < T < 170$, κ_π varied only by one or two percent from a value of 1.13.

During the course of the simulation, π_{zz} and F_π can be extracted from the momenta of the particles even when the system is not chemically equilibrated,

$$P = \frac{1}{V}\sum_{i\in V}\frac{p_i^2}{3E_i}, \tag{8}$$

$$\pi_{zz} = T_{zz} - P = \frac{1}{V}\sum_{i\in V}\frac{3p_{i,z}^2 - p_i^2}{3E_i},$$

$$F_\pi = \frac{1}{15V}\sum_{i\in V}\frac{p_i^4}{E_i^2},$$

$$\frac{F_\pi}{T} = P - \frac{1}{15V}\sum_{i\in V}\frac{p_i^4}{E_i^3}. \tag{9}$$

Given that F_π or F_π/T can be extracted from the cascade at any time rather easily and is essentially a known quantity, the relaxation time is not a free parameter if given the viscosity due to the Kubo relation, $\tau_\pi = \eta T/F_\pi$.

The last term in Eq. (2) has an unknown dimensionless coefficient γ_π. For kinetic theory of a massless gas with fixed cross sections and isotropic scattering, this coefficient is known to be 5/7 [33, 36, 37]. However, for this case we treat it as an unknown, so we are left with two free parameters to describe the evolution of π_{zz}. We then fit the behavior of the stress-energy tensor from a microscopic simulation performed in a controlled environment by varying both η and γ_π. Since this also fixes the relaxation time, τ_π, we can compare the relaxation time to the collision time and see whether $\tau_\pi \approx 2\tau_{\rm coll}$, which was found for the case studied in [33, 36].

Here, we initialize our microscopic simulation, B3D [40], with the longitudinally boost-invariant geometry of Bjorken hydrodynamics [41]. In this environment the only velocity gradient in the fluid frame is $\partial_z v_z = 1/\tau$, where $\tau = \sqrt{t^2 - z^2}$ is the proper time, the time relative to when the collision began according to an observer moving with the fluid. All the matter is situated at $z = 0$ at $\tau = 0$, due to the large Lorentz contraction of the incoming nuclei, then it flows with a collective velocity $v_z = z/t$. In the frame of the matter, the behavior of all intrinsic quantities, including the stress-energy tensor, is chosen to depend only on the proper time, making the evolution effectively invariant to longitudinal boosts for observers beginning at $z = t = 0$. The simulation B3D should behave similarly to the simulation URQMD which was used in [27]. The model B3D incorporates all the resonances in the particle data book [24] with masses $\lesssim 2$ GeV/c^2, a very similar list to the current version URQMD. For this study simple cross sections were used in B3D. In addition to the resonant cross sections for each species, a fixed cross section of 10 mb was added with particles scattering isotropically. Nonresonant cross sections in URQMD are calculated with the additive quark model [42], and tend to be somewhat larger than those used in B3D. In our simulations approximately 45% of the collisions were through the fixed cross section rather than through resonance formation. Resonances were formed according to the Breit-Wigner form described in the appendix, and decayed isotropically. A more realistic model would replace these $s-$wave decays with $p-$wave decays and would result in higher viscosities. True cross sections for the many hadronic species that are considered in B3D are unknown. If they are close to 30 mb, the scattering rate in B3D would be underestimating the scattering rate by $\sim 25\%$, which suggests that B3D might overstate the viscosity. If the $s-$ wave scatterings were replaced by $p-$ wave scatterings for the many cases where resonance formation is p-wave, the viscosity would probably increase by several tens of percent and the current version of B3D would be understating the viscosity. Thus, even in the limit of binary collisions model uncertainties are of the order of several tens of percent due to the lack of knowledge about scattering. It would not be surprising to learn that simple pictures like the one presented here mis-state the viscosity by that amount, though it would seem that these pictures should be valid to better than 50% as long as the temperatures are not so high that hadronic degrees of freedom become irrelevant.

Particles were initialized at a proper time τ_0 and temperature T_0, and with an initial anisotropy to the stress-energy tensor. The initial momenta were chosen according to the prescription in [43]. This code was modified relative to previous versions to initially generate particles with a distribution of masses consistent with a thermal-weighted modified Lorentzian distribution. This change is described in the appendix. The spatial coordinates were spread uniformly in spatial rapidity, $\eta_s = \sinh^{-1} z/\tau$, so that the intrinsic properties depended only on τ and not η. The extent of the simulation in the transverse direction was confined to a radius of $R = 40$ fm, with an extra buffer distance set up to ensure that the existence of the boundary could not affect the particles with radius $r < R$ during the finite time over which the cascade ran. The initial momentum

distribution was modified to reproduce arbitrary initial π_{zz} using the techniques of [43]. The distribution of the particles longitudinally was confined to spatial rapidities $-\eta_{s,\rm min} < \eta < \eta_{s\rm max}$, with cyclic boundary conditions to longitudinal boosts. The scattering algorithm in B3D was written in terms of τ and η and is explicitly invariant to longitudinal boosts. For instance, if collisions were ordered in the time t rather than the proper time τ, boost invariance could be violated. At high densities, cascade codes can differ from Boltzmann simulations due to the range of the interaction, $\sqrt{\sigma_\pi/\pi}$, extending to distances over which the collective velocity of the matter changes [44]. This can be corrected by oversampling the particles by a factor S, then reducing the cross sections by the same factor to ensure the collision rates are not changed. For this calculation a sampling factor $S = 4$ was applied for all calculations. Only the calculations at highest temperatures were noticeably affected by the oversampling.

Runs were first performed for four initial temperature, $T = 120, 135, 150$ and 165 MeV. To evaluate the behavior for a small velocity gradient, τ_0 was set to $1000, 750, 500$ and 250 fm/c. Larger values of τ_0 result in smaller viscous corrections, which then become increasingly difficult to analyze due to statistical noise. For these times the deviation π_{zz} was $\sim$ one percent of the pressure. Smaller τ_0 was used at higher temperature because the viscosities were smaller and using 1000 fm/c would have led to values of π_{zz} that were difficult to analyze due to statistical noise. The number of collisions and volumes were adjusted so that the typical number of analyzed particles would be on the order of 5×10^7 particles. At each time step, P, F_π and π_{zz} were determined by analyzing the particles momenta using Eq. (8). For each particle, the momenta in Eq. (8) were evaluated in the local rest frame of the fluid as determined by the particle's position. The entropy density is needed to determine α in Eq. (3) to parameterize the IS equations, and was taken by using the equilibrium entropy at τ_0 scaled down by τ_0/τ. This assumes entropy conservation during the expansion. Given the large number of hadronic species, which lose both local chemical and kinetic thermal equilibrium [45], a more sophisticated extraction of the entropy would be difficult, and given that the entropy is not expected to rise more than a few percent with these velocity gradients, this simple form for $s(\tau)$ should be sufficiently accurate given the other approximations inherent to the analysis. These quantities then determine both α and κ_π from Eq. (3). For each of the four initial temperatures, three simulations were performed with different initial values of $\pi_{zz}(\tau_0)$. The values were chosen to correspond to NS values of π_{zz} for $\eta/s = 0.08, 0.32$ and 1.28.

In the Bjorken geometry, the IS equations become

$$\begin{aligned} -\partial_\tau \pi_{zz} &= -\frac{1}{\tau_\pi}\left(\pi_{zz} - \frac{4\eta}{3\tau}\right) - \frac{\kappa_\pi}{\tau}\pi_{zz} - \frac{4\gamma_\pi}{3\tau}\pi_{zz}, \\ \partial_\tau\left(\frac{\pi_{zz}}{\alpha}\right) &= -\frac{1}{\tau'_\pi}\left(\frac{\pi_{zz}}{\alpha} - \frac{4\eta'}{3\alpha\tau}\right), \\ \tau'_\pi &= \tau_\pi/(1 + 4\gamma_\pi\tau_\pi/\tau), \\ \eta' &= \eta/(1 + 4\gamma_\pi\tau_\pi/\tau). \end{aligned} \tag{10}$$

The densities change modestly during the cascade, and thus both τ_π and γ_π might change slightly during the evolution. We assume that the relaxation time τ_π scales inversely with the hadron density, whereas γ_π is fixed. This approximation is based on the empirical fact that scattering rates tend to vary linearly with the density, especially for the modest changes seen here, and that the relaxation times should scale linearly with the collision time. The two varied parameters are then the initial values of τ_π and γ_π. The differential equation in Eq. (10) was then solved numerically, with the procedure repeated with different parameters varied until a best fit to the evolution was found.

The left-side panels of Fig. 1 show the fit of $\pi_{zz}(\tau)$ for the four temperatures described above with large initial τ_0. The IS equations reproduce both the relaxation of the stress-energy tensor toward the NS values, and the large τ behavior. For these small velocity gradients the effect of γ_π is negligible and one should extract the viscosity with confidence. The statistical noise in the extracted values are of the order of the size of the symbols in Fig. 1, with the noise being correlated between different neighboring points due to the finite time required for relaxation. At each temperature, the fits are convincing for reproducing the evolution for three initial conditions. Figure 2 shows the extracted viscosities from these fits both with $\gamma_\pi = 0.96$, and with $\gamma_\pi = 0$. For the small velocity gradients, the extracted values of the viscosity and relaxation times are nearly independent of γ_π. Also, the extracted relaxation time τ_π closely matches twice the collision time as extracted from the cascade. This contrasts with cascades for massless particles, where the result for isotropic cross sections is well known, both analytically [30] and numerically [29], where the ratio of the $\tau_\pi/\tau_{\rm coll} \approx 1.58$ is about 20% lower than what is found here. The hadronic case is far more complicated because particles are massive and collisions often involve the creation and decay of resonances.

To determine γ_π and to test the consistency of the approach, the procedure was repeated with large velocity gradients, by reducing τ_0 by a factor of 50, to values in the neighborhood of what one would encounter in central collisions of heavy ions when traversing the hadron gas region. Again, the procedure was repeated with $\gamma_\pi = 0$. Even though the fits to the evolution of π_{zz}, shown in the right-side panels of Fig. 3, were again successful, the extracted viscosity and relaxation time were different than the values extracted with large τ_0, or with small velocity gradients. Because τ_π was assumed to increase inversely with the hadron density, and because the hadron density falls approximately inversely with τ, the values for η' and τ'_π in Eq. (10) are effectively modified by a constant factor when γ_π is introduced. Thus, the fits in Fig. 1 are indistinguishable with or without γ_π, but the values of the viscosities and relaxation times differ. Fig. 2 shows the extracted viscosities as a function of temperature assuming $\gamma_\pi = 0$ and assuming $\gamma_\pi = 0.96$. For the value of

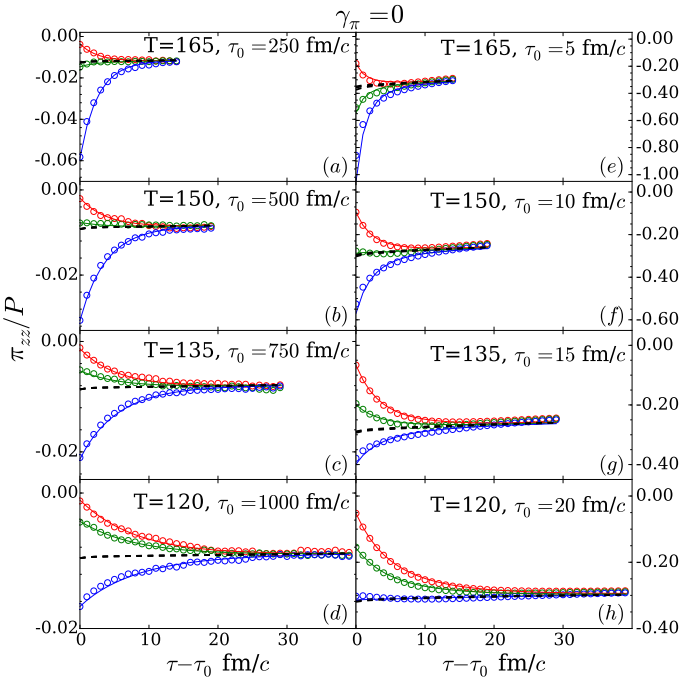

FIG. 1. (color online) The evolution of the stress-energy tensor as extracted from the hadronic simulation (circles) are compared to Israel-Stewart forms (solid lines) to extract effective viscosities. Each separate line corresponds to a different initialization of the deviation of the stress-energy tensor, π_{zz}. For larger times, the behavior approaches that of the Navier-Stokes equation (black dashed line). In the left-side panels (a-d) small velocity gradients were imposed, equivalently large τ_0, which should lead to true values of viscosity as τ_0 is much larger than the collision time. Only one parameter, the effective viscosity $\eta^{(\mathrm{eff})}$, was used to fit the three instances displayed for each panel, and the parameter γ_π was set to zero. If the assumption of linearity for the Navier-Stokes equation is valid, the same values of $\eta^{(\mathrm{eff})}$ would result from the right-side panels (e-h) which assume much larger velocity gradients, in the range of what might be produced in the environment of heavy-ion collisions.

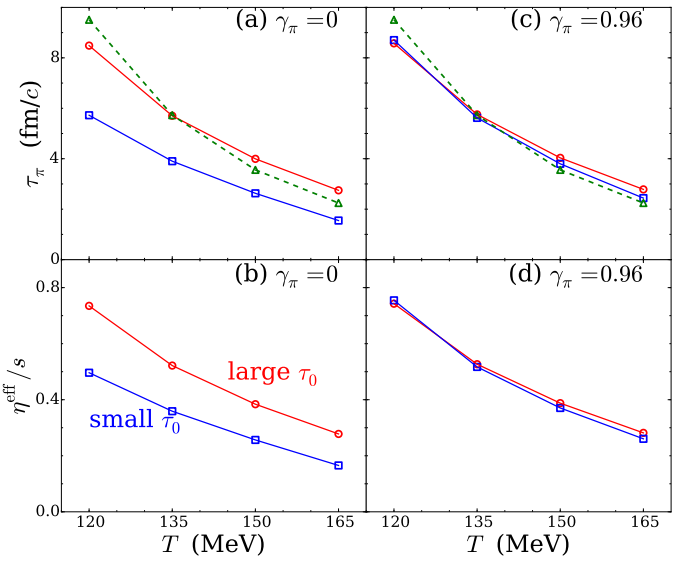

FIG. 2. (color online) The viscosity to entropy ratio extracted from calculations with small velocity gradients (red circles) differs from that calculated with large velocity gradients (blue circles), when one sets the viscous parameter $\gamma_\pi = 0$ as illustrated in panel (b). By setting the value $\gamma_\pi = 0.96$, the extracted viscosity becomes consistent for both velocity gradients as seen in panel (d). In the upper panels (a) and (c), the relaxation time τ_π is displayed, which mirrors the behavior of the viscosity. The extracted relaxation time in (c) consistently matches a value of two collision times, $2\tau_{\mathrm{coll}}$, which is represented by dashed lines.

0.96, the viscosities and relaxation times are nearly the same for the large and small values of τ_0.

To more strongly demonstrate the effect of $\gamma_\pi \neq 0$, several initial times were studied for the initial temperature $T_0 = 150$ MeV. The extracted viscosities are shown in Fig. 4, for both the case of $\gamma_\pi = 0$ and $\gamma_\pi = 0.96$. Effectively, the value of 0.96 was chosen by varying it until the viscosity in Fig. 4 was independent of τ_0.

III. DISCUSSION AND CONCLUSIONS

Given that the analyses based on small velocity gradients resulted in shear effects where π_{zz}/P is of the order of one percent, the extracted shear viscosities and relaxation times should be close to the correct values since higher-order viscous terms should be negligible. However, the conditions of heavy-ion collisions can be quite different in that shear corrections can easily be tens of percent. To test whether this procedure works equally well for larger velocity gradients, the method was repeated with much smaller values of τ_0, consistent with the scales inherent to where one samples the hadronic phase in heavy-ion collisions. By setting $\gamma_\pi = 0.96$, the extracted values of the viscosity are independent of the velocity gradient, even for conditions where π_{zz}/P is in the neighborhood of one third. This value for γ_π is higher than the value of 5/7 found for a gas of massless particles with fixed cross-section and isotropic scattering [36, 37]. Additionally, the IS coefficient κ_π was determined for a hadron gas, and found to be near 1.13. This is smaller than the value, 4/3, also determined in [36, 37], as expected given that the particles are massive.

The analyses seem robust given the ability of a few parameters to reproduce the stress-energy tensor for a wide range of temperatures, velocity gradients, and initial anisotropies of the stress-energy tensor. After extracting bulk quantities like F_π and collision rates from the simulations, only two parameters were varied for IS calculations to reproduce all evolutions for a given initial temperature. Those parameters were the shear relaxation time τ_π and the γ_π, which was fixed at 0.96 regardless of temperature. From Fig. 2, one could see that rather than choosing a different τ_π for each temper-

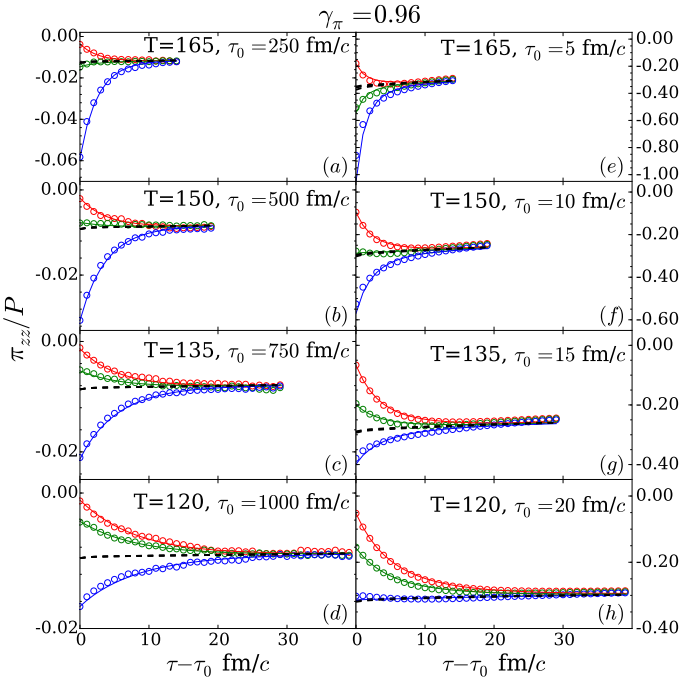

FIG. 3. (color online) The same as Fig. 1, only with $\gamma_\pi = 0.96$. The fits to the same evolutions of the stress-energy tensor are practically indistinguishable from Fig. 1 where γ_π was set to zero, but the extracted viscosities differed significantly for the cases with large velocity gradients, i.e. the small values of τ_0 used in the right-side panels (e-h).

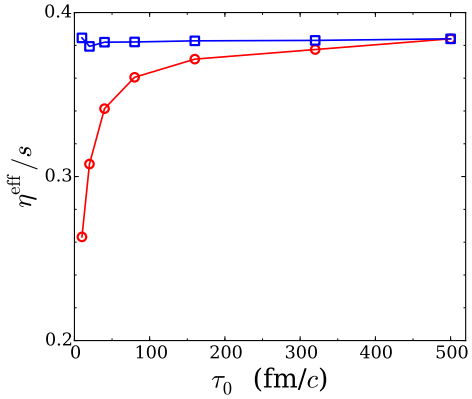

FIG. 4. (color online) The extracted viscosity to entropy ratio is shown for several runs which were all initialized with the same initial temperature, $T_0 = 150$ MeV, but had different initial velocity gradients, $1/\tau_0$. When setting $\gamma_\pi = 0$ (red circles), the extracted viscosity was sensitive to the initial velocity gradient, but with $\gamma_\pi = 0.96$ (blue squares), the results were independent of viscosity. This illustrates the importance of including the term in the Israel-Stewart equations for values of τ_0 in the neighborhood of those encountered in heavy-ion physics, $\sim 5 - 10$ fm/c.

ature, one could have chosen τ_π to be some factor multiplied by the collision time from the cascade. Thus, all 24 evolutions of π_{zz}/P from Fig. 2 could be reproduced by varying only two free parameters, $\gamma_\pi = 0.96$ and the ratio of $\tau_\pi/\tau_{\rm coll} = 2$.

These evolutions were matched both in reproducing the exponential decay of the initial anisotropy toward the NS evolution, and the magnitude of the NS evolution. For the cases with small velocity gradients, matching the exponential decay essential determines τ_π, whereas matching the asymptotic NS behavior simultaneously shows that the shear viscosity is matched. Matching the exponential decay for small velocity gradients essentially is similar to what is done in fixed-box geometries, such as in [27], in that extracting the exponential lifetime, combined with F_π, gives the viscosity. Given that the ratio of the shear viscosity to the relaxation time is F_π/T and is not a free parameter, because it can be extracted from the cascade or from a simple integral, this provides a consistency check to see that both the behavior of π_{zz}/P at early times, which is dominated by the exponential decay, and the behavior of π_{zz}/P at later times, which is determined by the viscosity in the NS equation, can be reproduced by a single parameter. Matching the behavior for the larger velocity gradients using the same parameters as for low velocity gradients required setting $\gamma_\pi \neq 0$. For $\gamma_\pi = 0.96$, the extracted viscosities shown in Fig. 4 were then independent of the size of the velocity gradients, at least up to the point where viscous corrections were on the order of one third of the pressure.

Unfortunately, we were unable to express γ_π analytically as was done for the massless case with fixed cross-sections and isotropic scattering in [36, 37]. For the complicated case considered here, where species have a variety of masses and collide with a variety of cross sections, heavier particles should require more collisions to lose memory of their momentum, and the stress-energy tensors should not be expected to relax according to a single relaxation time. Despite these difficulties, the coefficient κ_π could be expressed in terms of equilibrated phase space distributions, independently of any scattering properties. This was accomplished by enforcing the constraint that entropy must always rise, independent of whether the state of the stress-energy tensor. It would be interesting to see whether γ_π could also be expressed in a similar manner. It should not be forgotten that the coefficients τ_π, κ_π and γ_π are defined within the context of IS theory, which explicitly assumes the existence of a single exponential relaxation time. Thus, given that IS theory can only be considered as an effective theory once the velocity gradients become larger, the coefficients τ_π, κ_π and γ_π, are, at best, parameters of an effective theory

The bulk viscosity ζ, and the bulk corrections to the pressure, were neglected here. Due to the fact that a hadron gas includes both very relativistic particles, mainly the pions, and mostly non-relativistic particles, e.g. the baryons, the bulk viscosity is not negligible. However, stating the bulk viscosity requires comparing

the stress-energy tensor to the equilibrated values,

$$\Pi = (T_{xx} + T_{yy} + T_{zz})/3 - P. \tag{11}$$

In addition to the deviations of the momentum dependence of the phase space distributions, the yields of the various hadrons rapidly lose equilibrium in the cooling system, which also contributes to the bulk viscosity [46]. Thus, one must decide whether to include the contribution to Π from losing chemical equilibrium. Once the choice is made, it would be possible to follow the same procedure used here to determine ζ. However, the complexity of the chemistry would be difficult to track given the large number of different hadronic resonances.

Determining the transport coefficients of the hadronic phase might motivate one to replace the microscopic simulation, the cascade, with a hydrodynamic description. However, that would be naive. In addition to the shear corrections, the bulk corrections are complicated due to the lack of chemical equilibrium. The loss of kinetic equilibrium is mainly driven by the various mass states losing thermal contact and having both different local temperatures, and different collective flows [45, 47]. Applying a hydrodynamic picture to account for the large number of species all moving with different collective flows and different local temperatures is untenable.

The value of the viscosity near the boundary of the hadronic phase is, nonetheless, important. If one believes that the true values of both η and γ_π are close to those of the cascade, it would guide choosing those parameters near the interface. Typically, one would apply this interface near $T = 155$ MeV, the temperature where lattice calculations show that the hadron prescription begins to become unreasonable [48–50]. The guidance taken from this analysis contrasts with that of [27]. In this study, one would expect $\eta/s \approx 0.3$ once the temperature nears 160 MeV, whereas the viscosities in [27] had values $\eta/s \approx 1$ for all temperatures above 100 MeV as seen in Fig. 5. At low temperatures, the values found here are not far from those found in [20, 21] and [27], but differ increasingly as the temperature rises from that point. The fact that the temperature dependence of both the viscosity and relaxation time were consistent with relaxation requiring two collisions at any temperature, leads credence to the values found here, whereas the the nearly temperature-independent values of η/s extracted from the URQMD analysis in [27] are qualitatively at odds with expectations given that densities increase dramatically at higher temperatures, which should be accompanied by strongly falling collision times, and thus falling values of η/s. For temperatures near 160 MeV, the extracted viscosity from URQMD in [27] is four times higher than what was found here. The source of this discrepancy must come from some combination of increasing the shear relaxation time, τ_π, in URQMD relative to B3D or decreasing the collision rate. It would seem surprising that URQMD would have lower collision rates given that cross sections in URQMD are typically a bit larger. If collision rates are similar in the two models, the URQMD values for η/s would imply that the shear relaxation times would have to approach eight collision times to reproduce their values, which would also be surprising. Viscous effects from non-local scattering kernels, as discussed in [44], should not play a role in the URQMD analysis because it is performed in a static box geometry.

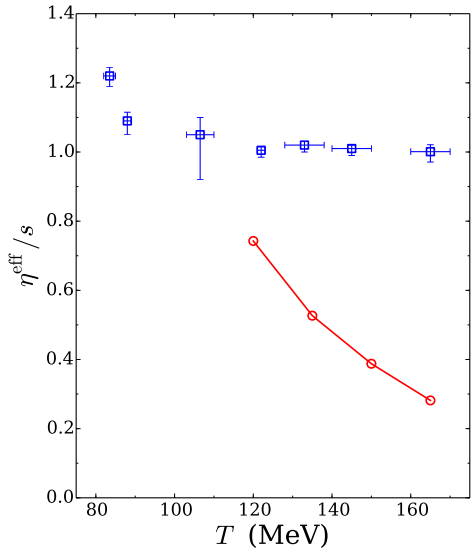

FIG. 5. (color online) Extracted viscosities from this analysis (red circles) are compared to those of the URQMD analysis in [27] (blue squares). For the calculations presented here, the fall of η/s with temperature is consistent with a relaxation time being twice the collision rate. In order to reproduce η/s from [27] when $T \approx 160$ MeV, the shear relaxation time, τ_π, would have to approach eight collision times, or the collision rate would have to be reduced by a factor of four.

Another lesson from this analysis is the importance of the term with γ_π in the IS equations, Eq. (2). Here, if one set $\gamma_\pi = 0$, the extracted viscosity would have been understated by $\sim 30\%$ for calculations with velocity gradients having strengths characteristic of heavy-ion collisions. The statistical analysis of RHIC and LHC data in [51] indeed applied an IS hydrodynamic picture with $\gamma_\pi = 0$. Because the physics of elliptic flow is driven by the stress-energy tensor, and if those anisotropies could be reproduced by calculations with higher viscosity if γ_π was not set to zero, the extracted viscosities might be significantly larger, perhaps by a few tens of percent if γ_π were set to a reasonable value. If that were the case, the value of the viscosity for matter just above the interface temperature, might have been found to be nearer to three to four times the AdS/CFT limit, $\eta/s = 1/4\pi$, rather than the two to three times that was found in the global analysis in [51].

If complex global analyses indeed converge on viscosities of the QGP being in the range of three to four times $1/4\pi$, the values would be consistent with those extracted here from B3D for temperatures $\gtrsim 160$ MeV. However, it should be emphasized that hadronic simulations become increasingly questionable as temperatures rise above 150

MeV. This would suggest that viscosities in the QGP approach that of a hadron gas for temperatures in the transition region, and would also be similar to values from recent lattice calculations [11], which also have rather high uncertainties. Perturbation theory does predict significantly higher viscosities [13], which suggests that the non-perturbative nature of QCD matter continues for energy densities significantly higher than the transition region, $150 \lesssim T \lesssim 220$ MeV.

In this work, we have studied transport properties in the hot hadron gas by measuring the energy-momentum tensor in a hadron cascade simulation undergoing longitudinal expansion. We were able to extract a temperature dependent value of the shear viscosity over entropy density for temperature between 120 and 170 MeV. We were able to extract an estimate for the shear viscous relaxation time for temperatures between 120 and 165 MeV, along with the transport coefficients τ_π, κ_π and γ_π that appear in IS theory. This work sheds some light on what one might expect for these coefficients in nature, though with significant uncertainty given the crude nature of the cascade and the uncertainties in scattering. If one had a better determination of these coefficients from a more fundamental theory, this work might also provide the insight necessary to adjust the cascade to behave consistently with the desired transport coefficients.

Appendix: Constraining Israel Stewart Eq.s from Linear Response Theory

Israel-Stewart (IS) equations differ from Navier-Stokes (NS) equations by treating the spatial components of the stress-energy tensor as dynamical variables. First, we use shorthand to define the spatial components of the stress-energy tensor and the velocity gradients,

$$
\begin{aligned}
a_1 &\equiv \frac{1}{2}(T_{xx} - T_{yy}), && \text{(A.1)}\\
a_2 &\equiv \frac{1}{\sqrt{12}}\left(T_{xx} + T_{yy} - 2T_{zz}\right),\\
a_3 &\equiv T_{xy}, \quad a_4 \equiv T_{xz}, \quad a_5 \equiv T_{yz},\\
b &\equiv \frac{1}{3}\left(T_{xx} + T_{yy} + T_{zz}\right) - P,\\
\omega_1 &\equiv \partial_x v_x - \partial_y v_y, && \text{(A.2)}\\
\omega_2 &\equiv \frac{1}{\sqrt{3}}\left(\partial_x v_x + \partial_y v_y - 2\partial_z v_z\right),\\
\omega_3 &\equiv \partial_x v_y + \partial_y v_x, \quad \omega_4 \equiv \partial_x v_z + \partial_z v_x, \quad \omega_5 \equiv \partial_y v_z + \partial_z v_y.
\end{aligned}
$$

With these definitions the NS equations become

$$a_i = -\eta\omega_i, \quad b = -\zeta\nabla\cdot v, \tag{A.3}$$

where η and ζ are the shear and bulk viscosities respectively, and the rate of work being done per unit volume is

$$\sum_i a_i\omega_i + (P+b)\nabla\cdot v = \sum_{ij} T_{ij}\partial_i v_j. \tag{A.4}$$

Assuming exponential decay of the correlations of the stress-energy tensor, the Kubo relations are

$$
\begin{aligned}
\eta &= \frac{\tau_\pi}{T}F_\pi, \quad \zeta = \frac{\tau_\Pi}{T}F_\Pi, && \text{(A.5)}\\
F_\pi &= \int d^3r\,\langle a_j(0)a_j(\mathbf{r})\rangle\,, \quad F_\Pi = \int d^3r\,\langle b(0)b(\mathbf{r})\rangle\,.
\end{aligned}
$$

The indices j are not summed. The quantities F_π and F_Π describe the equal-time fluctuations of the tensor at equilibrium. For a gas equal-time correlations vanish except between a particle and itself. The shear correlations can then be calculated in either discrete or differential form

$$
\begin{aligned}
F_\pi &= \frac{1}{V}\sum_{i\in V}\frac{p_{i,x}^2 p_{i,y}^2}{E_i^2}, && \text{(A.6)}\\
&= \sum_k (2S_k+1)\int\frac{d^3p}{(2\pi)^3}e^{-E_k(p)/T}\frac{p_x^2p_y^2}{E_k(p)^2},\\
&= \frac{1}{30\pi^2}\sum_k (2S_k+1)\int\frac{p^6dp}{E_k(p)^2}e^{-E_k(p)/T},\\
\frac{F_\pi}{T} &= P - \frac{1}{30\pi^2}\sum_k (2S_k+1)\int\frac{p^6dp}{E_k(p)^2}e^{-E_k(p)/T}.
\end{aligned}
$$

The sum over k describes a sum over all the species of the hadron gas with spins S_k. These quantities can be calculated as a function of the temperature for a thermalized system from the integral, and can be determined from the simulation in a non-thermalized system using the discrete sum. The bulk term F_Π is small for a gas, and vanishes for either massless particles or for non-relativistic particles. We neglect it here. Given that F_π is known, extracting the shear viscosity comes down to determining the relaxation time τ_π.

In the matter frame, the IS equations have the form

$$
\begin{aligned}
\partial_t\pi_{ij} = -\frac{1}{\tau_\pi}\left\{\pi_{ij} - \eta\omega_{ij}\right\} - \kappa_\pi\pi_{ij}\nabla\cdot v \qquad \text{(A.7)}\\
-\gamma_\pi\pi_{ik}\omega_{kj}.
\end{aligned}
$$

Terms of higher order in the deviations, e.g. π^2 are neglected as this is considered an expansion in the inverse Reynolds number [36]. Terms of higher order derivatives, e.g. ω^2, involve non-local effects and should also be much smaller. In addition, such terms make the equations non-parabolic and can lead to super-luminar transport. At non-zero baryon density or if one considers bulk corrections, one must add additional terms that involve b and fluctuations of the charge density.

For the immediate purpose, we neglect the 2nd-order term with γ_π. This term is known to be important [39], but is not needed for the following proof. After setting $\gamma_\pi = 0$ in Eq. (A.7), the IS equations can be written as

$$\partial_t\left(\frac{a_i}{\alpha}\right) = -\frac{1}{\tau_\pi}\left(\frac{a_i}{\alpha} - \frac{a_i^{(\mathrm{NS})}}{\alpha}\right), \tag{A.8}$$

where α is some function of the temperature, related to κ_π by

$$\kappa_\pi \nabla \cdot v = -\frac{1}{\alpha}\partial_t \alpha \tag{A.9}$$

$$\kappa_\pi = \frac{s}{\alpha}\partial_s \alpha, \tag{A.10}$$

where the last step used conservation of entropy, $\partial_t s = -s\nabla \cdot v$.

In the next few lines we show that

$$\alpha^2 = F_\pi s, \tag{A.11}$$

by applying the constraint that the entropy must always rise, regardless of the signs of either the deviations of the stress-energy tensor, a_i or b, or of the velocity gradients, ω_i or $\nabla \cdot v$.

The entropy of a volume V for deviations of the anisotropy of the stress-energy tensor at fixed energy is

$$S = sV - \frac{1}{2}sV\sum_i \frac{a_i^2}{F_\pi s}, \tag{A.12}$$

ignoring the fluctuation of the bulk component for the moment.The appearance of F_π ensures that the average $\langle a_i^2 \rangle$, where the averaging is with the weight e^S within a large volume, returns F_π/V. The rate of change of entropy production, including that due to changing a_i is

$$\frac{dS}{dt} = -\frac{V}{T}\sum_i a_i\omega_i - s\frac{a_i}{\sigma_\pi}\frac{d}{dt}\frac{a_i}{\sigma_\pi}, \tag{A.13}$$
$$\sigma_\pi^2 \equiv F_\pi s.$$

We have made use of the fact that the term sV can be considered a constant here because entropy is nearly conserved, and the term is already being multiplied by a_i^2, which is already small. The first term accounts for the rise of the entropy of s due to the rise of the energy of the expansion in a system where $\nabla \cdot v = 0$, and comes from the thermodynamic relation, Eq. (A.4). One can now insert the IS ansatz, Eq. (A.8), into Eq. (A.13) and find

$$\begin{aligned}\frac{dS}{dt} &= -V\sum_i \left\{ \frac{1}{T}a_i\omega_i - s\frac{a_i\alpha}{\sigma_\pi^2\tau_\pi}\left(\frac{a_i}{\alpha} + \frac{\eta\omega_i}{\alpha}\right) \right. \\ &\quad \left. + s\frac{a_i^2}{\sigma_\pi\alpha}\frac{d}{dt}\left(\frac{\alpha}{\sigma_\pi}\right)\right\} \\ &= \frac{sV}{\tau_\pi\sigma_\pi^2}\sum_i a_i^2 - V\left(\frac{1}{T} - \frac{s\eta}{\sigma_\pi^2}\right)\sum_i a_i\omega_i, \\ &\quad + sV\frac{a_i^2}{\sigma_\pi\alpha}\frac{d}{dt}\left(\frac{\alpha}{\sigma_\pi}\right)\end{aligned} \tag{A.14}$$

The Kubo relation, Eq. (A.5), ensures the middle term vanishes. The last term must vanish whether the ratio α/σ_π is rising or falling, to ensure that the entropy always increases. This implies that α and σ_π are equal to within an arbitrary constant factor. Thus $\alpha^2 = \sigma_\pi^2 = F_0 s$, and

$$\frac{dS}{dt} = \frac{V}{F_\pi\tau_\pi}\sum_i a_i^2 = \frac{V}{T\eta}\sum_a a_i^2. \tag{A.15}$$

If the stress-energy tensor relaxes to the NS value, $a_i = -\eta\omega_i$, entropy production approaches the usual value $dS/dt = (\eta V/T)\sum_i \omega_i^2$. The corresponding expressions for the bulk contributions involve $a_i \to b$ and $\omega_i \to \nabla \cdot v$.

Finally, we rewrite the IS equations in a form that can be compared to other work, in this case a massless gas expanding in a Bjorken geometry [32]. Equation (4) can be expressed as

$$\frac{d}{dt}a_i = -\frac{1}{\tau_\pi}\left(a_i - a_i^{(\mathrm{NS})}\right) + \frac{a_i}{\alpha}\frac{d}{dt}\alpha. \tag{A.16}$$

For a massless gas α scales like the energy density and falls with the proper time as $\tau^{-4/3}$ so $\dot{\alpha}\alpha = -4/3\tau$, and

$$\frac{d}{dt}a_i = -\frac{1}{\tau_\pi}\left(a_i - a_i^{(\mathrm{NS})}\right) - \frac{4}{3}\frac{a_i}{\tau}. \tag{A.17}$$

This agrees with the corresponding expression in [36, 37]. Finally, one can reintroduce the term proportional to $\omega\pi$ in Eq. (A.7) and get

$$\frac{d}{dt}\pi_{zz} = -\frac{1}{\tau_\pi}\left(\pi_{zz} - \pi_{zz}^{(\mathrm{NS})}\right) - \frac{4}{3}\frac{\pi_{zz}}{\tau} - \frac{4\gamma_\pi}{3}\frac{\pi_{zz}}{\tau} \tag{A.18}$$

In [36, 37], the factor γ_π was found to be 5/7 for a gas of massless particle with fixed cross sections and isotropic scattering, whereas our best fit here gave $\gamma_\pi \approx 0.96$.

Although we ignore bulk corrections to the pressure, $b = (T_{xx} + T_{yy} + T_{zz})/3 - P$, the same derivation above can be extended to include the bulk viscosity. In that case, the IS equations become

$$\begin{aligned}\partial_\tau \pi_{ij} &= -\frac{1}{\tau_\pi}\left(\pi_{ij} - \eta\omega_{ij}\right) - \kappa_\pi\pi_{ij}\nabla\cdot v - \gamma_\pi\pi_{ik}\omega_{kj} - Jb\omega_{ij}, \\ \partial_\tau b &= -\frac{1}{\tau_b}\left(b - \zeta\nabla\cdot v\right) - \kappa_b b\nabla\cdot v - K\mathrm{Tr}\ \pi\omega.\end{aligned} \tag{A.19}$$

The same entropy arguments used for the evolution of π_{ij}, can be applied above to give

$$\begin{aligned}F_\Pi &= \int d^3r b(0)b(r), \\ \zeta &= \tau_b F_\Pi/T, \\ \beta^2 &= F_\Pi s, \\ \kappa_\Pi &= s\frac{\partial_s\beta}{\beta}, \\ JF_\Pi &= KF_\pi.\end{aligned} \tag{A.20}$$

Thus, given F_Π, there are two additional independent parameters if one includes the bulk viscosity: the bulk viscosity ζ, and either J or K.

Appendix: Generating Initial Thermal Masses

In order to instantiate the cascade B3D, particles are generated consistently with their distributions in a thermalized system. However, the previous version of B3D

had a shortcoming, in that particles were initially assigned their pole mass, rather than a distribution consistent with the spectral function. In this study a mass distribution, or spectral function $S(M)$, was implemented with the form of a modified Lorentzian,

$$\frac{dN}{dM} = S(M) = \frac{2}{\Gamma_R \pi} \frac{(\Gamma/2)^2}{(M - M_R)^2 + (\Gamma/2)^2}, \quad \text{(A.1)}$$
$$\Gamma = \Gamma_R \left(\frac{2k^2}{k_R^2 + k^2} \right)^{\alpha}.$$

Here, k is the momentum of one of the particles in the center-of-mass frame where their momenta are $\vec{k}$ and $-\vec{k}$. The parameter α was chosen to be $1/2$, but a more realistic model could have chosen different values depending on the angular momentum of the resonance. The momentum required to reach the resonance energy, M_R, is k_R. The cross section for creating a resonance was chosen to have the form,

$$\sigma = \frac{4\pi}{k^2} \frac{(\Gamma/2)^2}{(M - M_R)^2 + (\Gamma/2)^2}, \quad \text{(A.2)}$$

and the lifetime of the resonance was chosen to be Γ_R, independent of the off-shellness. One can calculate the fraction of time spent in the resonance for particles of that energy in a volume V by multiplying the collision rate and the lifetime,

$$f_R = \frac{\sigma v_{\text{rel}}}{\Gamma_R V}, \quad \text{(A.3)}$$

where $v_{\text{rel}} = |v_1| + |v_2|$ is the relative velocity. According to the Ergodic theorem [52], this should be the ratio of the spectral function to the density of states in the continuum,

$$\frac{S(M)}{dN_{\text{cont}}/dM} = \frac{S(M)}{(2\pi)^{-3} 4\pi k^2/(dM/dk)}. \quad \text{(A.4)}$$

Since $dM/dK = dE_1/dk + dE_2/dk = |v_1| + |v_2|$, one can see that this ratio indeed equals f_R, and the method is ergodically consistent. If a system is created in a box with this mass distribution, that mass distribution should remain the same throughout time due this consistency. However, due to the fact that the inverse processes for three-body decays are missing from B3D, and because for multichannel systems the mass distribution is calculated using only the principal decay channel, the system properties might relax somewhat away from those of the system immediately after creation.

Given the spectral function, the densities of each species are found by integrating over the densities of possible masses weighted by $S(M)$. Once the decision has been made to create a given species, masses are first chosen according to $S(M)$. This tends to skew the choice toward masses above M_r due to the momentum dependence of the width, unless $\alpha = 0$, and due to the fact that the lower end of masses is cut off due to kinematics, M must be greater than the sum of the two decaying masses $m_1 + m_2$. The mass M is then kept or rejected proportional to the density of particles with that mass. This thermal weighting then skews the mass downwards. The average masses can then be either greater or less than M_r depending on how much larger M is relative to $m1$ and m_2, the choice of α, and the temperature. Figure 6 shows how the energy density and speed of sound are changed by this procedure compared to generating all particles with their pole mass. Energy densities are lowered by $\sim 3\%$ at higher temperatures, and the speed of sound is raised by a few percent.

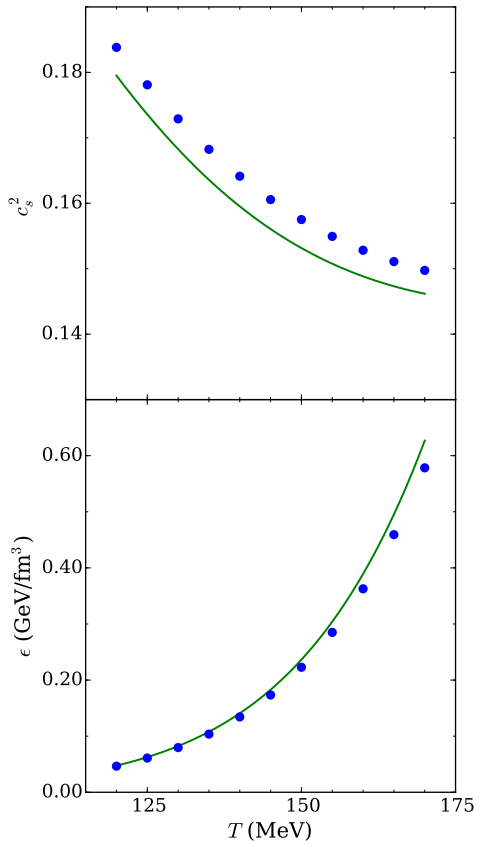

FIG. 6. (color online) Compared to using the pole mass (green line) to calculate densities of resonances, the altered equation of state from the spectral function in Eq. (A.1) (blue points) is somewhat stiffer, with energy densities lowered by a few percent and the speed of sound raised by a few percent.

ACKNOWLEDGMENTS

This work was supported by the Department of Energy Office of Science, awards No. DE-SC0008132 and DE-FG02-03ER41259. Alexander Baez acknowledges support from the National Science Foundation, Research Experience for Undergraduates, Division of Physics, award no. 1559866, and Jane Kim was supported by the Director's Research Scholar Program at the National Superconducting Cyclotron Laboratory, funded by the Na-

tional Science Foundation through award no. 1102511. The authors thank Paul Romatschke for valuable discussions and helping with writing the manuscript.

[1] Y. Aoki, G. Endrodi, Z. Fodor, S. Katz, and K. Szabo, Nature **443**, 675 (2006), hep-lat/0611014.
[2] T. Bhattacharya, M. I. Buchoff, N. H. Christ, H. T. Ding, R. Gupta, et al. (2014), 1402.5175.
[3] P. Romatschke and U. Romatschke, Phys. Rev. Lett. **99**, 172301 (2007), 0706.1522.
[4] H. Song and U. W. Heinz, J. Phys. **G36**, 064033 (2009), 0812.4274.
[5] J. E. Bernhard, P. W. Marcy, C. E. Coleman-Smith, S. Huzurbazar, R. L. Wolpert, and S. A. Bass, Phys. Rev. **C91**, 054910 (2015), 1502.00339.
[6] J. E. Bernhard, J. S. Moreland, S. A. Bass, J. Liu, and U. Heinz, Phys. Rev. **C94**, 024907 (2016), 1605.03954.
[7] E. Sangaline and S. Pratt, Phys. Rev. **C93**, 024908 (2016), 1508.07017.
[8] P. Kovtun, D. T. Son, and A. O. Starinets, Phys. Rev. Lett. **94**, 111601 (2005), hep-th/0405231.
[9] F. Karsch and H. W. Wyld, Phys. Rev. **D35**, 2518 (1987).
[10] H. B. Meyer, Phys. Rev. Lett. **100**, 162001 (2008), 0710.3717.
[11] S. W. Mages, S. Borsnyi, Z. Fodor, A. Schaefer, and K. Szabo, PoS **LATTICE2014**, 232 (2015).
[12] A. Nakamura and S. Sakai, Phys. Rev. Lett. **94**, 072305 (2005), hep-lat/0406009.
[13] P. B. Arnold, G. D. Moore, and L. G. Yaffe, JHEP **05**, 051 (2003), hep-ph/0302165.
[14] S. Gavin, Nucl.Phys. **A435**, 826 (1985).
[15] M. Prakash, M. Prakash, R. Venugopalan, and G. Welke, Phys.Rept. **227**, 321 (1993).
[16] A. Dobado and S. N. Santalla, Phys.Rev. **D65**, 096011 (2002), hep-ph/0112299.
[17] J.-W. Chen and E. Nakano, Phys.Lett. **B647**, 371 (2007), hep-ph/0604138.
[18] J.-W. Chen, Y.-H. Li, Y.-F. Liu, and E. Nakano, Phys.Rev. **D76**, 114011 (2007), hep-ph/0703230.
[19] K. Itakura, O. Morimatsu, and H. Otomo, Phys.Rev. **D77**, 014014 (2008), 0711.1034.
[20] A. Wiranata and M. Prakash, Phys.Rev. **C85**, 054908 (2012), 1203.0281.
[21] A. Wiranata, V. Koch, M. Prakash, and X. N. Wang, Phys.Rev. **C88**, 044917 (2013), 1307.4681.
[22] C. Sasaki and K. Redlich, Nucl. Phys. **A832**, 62 (2010), 0811.4708.
[23] P. Chakraborty and J. I. Kapusta, Phys. Rev. **C83**, 014906 (2011), 1006.0257.
[24] K. A. Olive, Chin. Phys. **C40**, 100001 (2016).
[25] S. Muroya and N. Sasaki, Prog. Theor. Phys. **113**, 457 (2005), nucl-th/0408055.
[26] S. Bass, M. Belkacem, M. Bleicher, M. Brandstetter, L. Bravina, et al., Prog.Part.Nucl.Phys. **41**, 255 (1998), nucl-th/9803035.
[27] N. Demir and S. A. Bass, Phys.Rev.Lett. **102**, 172302 (2009), 0812.2422.
[28] H. Song, S. A. Bass, and U. Heinz, Phys.Rev. **C83**, 024912 (2011), 1012.0555.
[29] C. Wesp, A. El, F. Reining, Z. Xu, I. Bouras, and C. Greiner, Phys. Rev. **C84**, 054911 (2011), 1106.4306.
[30] S. de Groot, W. van Leeuwen, and van Weert Ch. G., *Relativistic Kinetic Theory, Principles and Applications* (North- Holland, Amsterdam, 1980).
[31] A. Muronga, Phys. Rev. **C69**, 034903 (2004), nucl-th/0309055.
[32] G. S. Denicol, T. Koide, and D. H. Rischke, Phys. Rev. Lett. **105**, 162501 (2010), 1004.5013.
[33] G. Denicol, E. Molnr, H. Niemi, and D. Rischke, Eur.Phys.J. **A48**, 170 (2012), 1206.1554.
[34] G. S. Denicol, U. W. Heinz, M. Martinez, J. Noronha, and M. Strickland, Phys. Rev. Lett. **113**, 202301 (2014), 1408.5646.
[35] G. D. Moore and K. A. Sohrabi, Phys. Rev. Lett. **106**, 122302 (2011), 1007.5333.
[36] G. S. Denicol, H. Niemi, E. Molnar, and D. H. Rischke, Phys. Rev. **D85**, 114047 (2012), [Erratum: Phys. Rev.D91,no.3,039902(2015)], 1202.4551.
[37] D. Bazow, U. W. Heinz, and M. Strickland, Phys. Rev. **C90**, 054910 (2014), 1311.6720.
[38] G. S. Denicol, U. W. Heinz, M. Martinez, J. Noronha, and M. Strickland, Phys. Rev. **D90**, 125026 (2014), 1408.7048.
[39] D. Bazow, U. W. Heinz, and M. Strickland (2016), 1608.06577.
[40] J. Novak, K. Novak, S. Pratt, C. Coleman-Smith, and R. Wolpert (2013), 1303.5769.
[41] J. D. Bjorken, Phys. Rev. **D27**, 140 (1983).
[42] M. Bleicher et al., J. Phys. **G25**, 1859 (1999), hep-ph/9909407.
[43] S. Pratt and G. Torrieri, Phys.Rev. **C82**, 044901 (2010), 1003.0413.
[44] S. Cheng, S. Pratt, P. Csizmadia, Y. Nara, D. Molnar, M. Gyulassy, S. E. Vance, and B. Zhang, Phys. Rev. **C65**, 024901 (2002), nucl-th/0107001.
[45] S. Pratt and J. Murray, Phys. Rev. **C57**, 1907 (1998).
[46] K. Paech and S. Pratt, Phys. Rev. **C74**, 014901 (2006), [Erratum: Phys. Rev.C93,no.5,059902(2016)], nucl-th/0604008.
[47] H. Sorge, Phys. Lett. **B373**, 16 (1996), nucl-th/9510056.
[48] R. Bellwied, S. Borsanyi, Z. Fodor, S. D. Katz, A. Pasztor, C. Ratti, and K. K. Szabo, Phys. Rev. **D92**, 114505 (2015), 1507.04627.
[49] S. Borsanyi, Z. Fodor, S. D. Katz, S. Krieg, C. Ratti, and K. Szabo, JHEP **01**, 138 (2012), 1112.4416.
[50] A. Bazavov et al. (HotQCD), Phys. Rev. **D86**, 034509 (2012), 1203.0784.
[51] S. Pratt, E. Sangaline, P. Sorensen, and H. Wang, Phys. Rev. Lett. **114**, 202301 (2015), 1501.04042.
[52] P. Danielewicz and S. Pratt, Phys. Rev. **C53**, 249 (1996), nucl-th/9507002.